



Magnetocaloric effect of $\text{Fe}_{25}\text{Co}_{25}\text{Ni}_{25}\text{Mo}_5\text{P}_{10}\text{B}_{10}$ high-entropy bulk metallic glass



ARTICLE INFO

Keywords:

High-entropy alloy
Bulk metallic glass
Magnetocaloric effect
High-entropy effect

ABSTRACT

In this work, $\text{Fe}_{25}\text{Co}_{25}\text{Ni}_{25}\text{Mo}_5\text{P}_{10}\text{B}_{10}$ high-entropy bulk metallic glass (HE-BMG) with a maximum diameter of 1.2 mm is prepared by combining fluxing treatment and J-quenching technique. The magnetocaloric effect and the “high-entropy effect” on the magnetocaloric properties of the present $\text{Fe}_{25}\text{Co}_{25}\text{Ni}_{25}\text{Mo}_5\text{P}_{10}\text{B}_{10}$ HE-BMG have been investigated. The Curie temperature of the present $\text{Fe}_{25}\text{Co}_{25}\text{Ni}_{25}\text{Mo}_5\text{P}_{10}\text{B}_{10}$ HE-BMG is 560 K, the peak value of the magnetic entropy change and the refrigerant capacity are $0.80 \text{ J kg}^{-1} \text{ K}^{-1}$ and 135.4 J kg^{-1} under the applied field of 1.5 T, $1.88 \text{ J kg}^{-1} \text{ K}^{-1}$ and 310.2 J kg^{-1} under the applied field of 5 T, respectively. Compared with other transition metal-based BMGs, the present $\text{Fe}_{25}\text{Co}_{25}\text{Ni}_{25}\text{Mo}_5\text{P}_{10}\text{B}_{10}$ HE-BMG does not exhibit a relatively larger magnetic entropy change but a much wider full width at half maximum temperature of the magnetic entropy change curve, thus a larger refrigerant capacity.

1. Introduction

The development of magnetic refrigeration materials with excellent magnetocaloric performance is a key issue of magnetic refrigeration technology. Amorphous alloy is a new type of metal material, its atomic arrangement structure is long-range disorder, with no grain and grain boundaries [1]. In recent years, many studies have shown that amorphous alloys exhibit unique advantages in magnetic refrigeration. Firstly, amorphous materials with secondary phase transitions have greater stability in the refrigeration cycle than traditional crystalline materials [2]. Secondly, the disordered structure of the amorphous alloy results in a smaller thermal conductivity and a high electrical resistance, which is advantageous for reducing heat conduction and eddy current loss during magnetic refrigeration [3]. Finally, due to the disordered amorphous structure, its magnetic transition has a wide temperature range, so it has a large cooling capacity [4].

High-entropy alloy (HEA) is a new type of alloy, which contains five or more main elements in equal or near-equal atomic percent ranging from 5 to 35 at.% [5]. Because of their multiple compositions, complicated microstructures, and adjustable properties, HEA had attracted increasing research interests in both fundamental sciences and engineering applications [6–10]. Further, due to the unique topology and chemical chaotic structure, high-entropy bulk metallic glasses (HE-BMGs) exhibit many excellent properties compared with ordinary bulk metallic glasses (BMGs) and high-entropy alloys (HEAs). $\text{Zn}_{20}\text{Ca}_{20}\text{Sr}_{20}\text{Yb}_{20}(\text{Li}_{0.55}\text{Mg}_{0.45})_{20}$ [11] and SrCaYbLiMgZn [12] HE-BMGs exhibit ultra-low glass transition temperature and significant uniform plastic deformation at room temperature. $\text{Ca}_{20}\text{Mg}_{20}\text{Zn}_{20}\text{Sr}_{20}\text{Yb}_{20}$ HE-BMG has better mechanical properties and corrosion resistance. Compared with CaMgZn BMGs, and thus is more suitable for biomedicine [9]. However, so far little research has been done on the magnetic properties, especially magnetocaloric properties, of high-entropy bulk metallic glasses. Magnetic refrigeration technology is based on the magnetocaloric effect of magnetic refrigerant materials. The magnetocaloric effect is closely related to the magnetic entropy and lattice entropy of the material [13]. Therefore, it will be a

worthy and interesting topic whether the high-configuration entropy has a significant contribution to the magnetocaloric properties of HE-BMG. Until now, the relevant research has only been done on the rare earth (RE)-based HE-BMGs [14,15]. Compared with RE-based BMGs, transition metal (TM = Fe, Co and Ni) based BMGs have unique advantages in application of magnetic refrigeration due to the excellent magnetocaloric properties and relatively low cost [16]. In this work, a novel TM-based HE-BMG of $\text{Fe}_{25}\text{Co}_{25}\text{Ni}_{25}\text{Mo}_5\text{P}_{10}\text{B}_{10}$ has been prepared. The magnetocaloric effect of the present $\text{Fe}_{25}\text{Co}_{25}\text{Ni}_{25}\text{Mo}_5\text{P}_{10}\text{B}_{10}$ HE-BMG is investigated and high entropy effect on its magnetocaloric properties is explored.

2. Experimental

$\text{Fe}_{25}\text{Co}_{25}\text{Ni}_{25}\text{Mo}_5\text{P}_{10}\text{B}_{10}$ alloy ingot was prepared from Fe powder (99.9% pure), Co powder (99.9% pure), Ni powder (99.7% pure), Fe_3P powder (99.5% pure), Mo powder (99.7% pure) and B piece (99.9% pure). After the right proportion was weighed, they were put in a clean fused silica tube and alloying was brought about by torch under a high-purity Ar atmosphere. All the as-prepared alloy ingots had a mass of 1–2 g. Subsequently, the as-prepared alloy ingot was fluxed in a fluxing agent composed of B_2O_3 and CaO with the mass ratio of 3:1 at an elevated temperature under a vacuum of $\sim 50 \text{ Pa}$ for 4 h. After fluxed treatment, the alloy ingots were cooling down to ambient temperature and then subjected to J-quenching technique. As a result, $\text{Fe}_{25}\text{Co}_{25}\text{Ni}_{25}\text{Mo}_5\text{P}_{10}\text{B}_{10}$ alloy rods with a diameter of 1–1.2 mm and a length of 5–8 cm had been prepared.

The amorphous nature of the as-prepared samples was confirmed by X-ray diffractometer (XRD, Bruker D8 Advance). The thermal behavior of the as-prepared specimens was examined by differential scanning calorimetry (DSC, NETZSCH DSC 404F1) at a heating rate of 0.33 K/s under an Ar atmosphere. The magnetocaloric properties of the samples were measured by using a SQUID magnetometer (SQUID, MPMS XL-7).

<https://doi.org/10.1016/j.jmmm.2019.165404>

Received 19 February 2019; Received in revised form 3 May 2019; Accepted 3 June 2019

Available online 03 June 2019

0304-8853/© 2019 Elsevier B.V. All rights reserved.

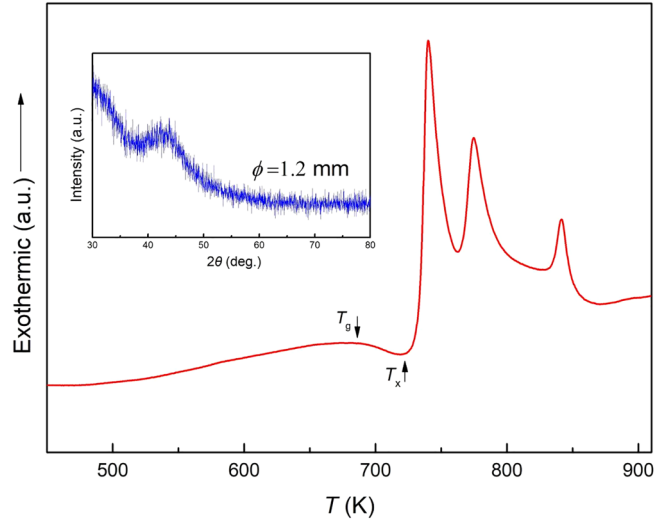


Fig. 1. XRD (inset) and DSC curves of the as-prepared $\text{Fe}_{25}\text{Co}_{25}\text{Ni}_{25}\text{Mo}_5\text{P}_{10}\text{B}_{10}$ HE-BMG.

3. Results and discussion

Fig. 1 shows the XRD pattern and DSC curve of as-prepared $\text{Fe}_{25}\text{Co}_{25}\text{Ni}_{25}\text{Mo}_5\text{P}_{10}\text{B}_{10}$ high-entropy alloy rod with a diameter of 1.2 mm. The XRD pattern of the sample shows a typical diffuse peak and no sharp crystalline peaks, indicating the fully glassy phase formation. The DSC curve of the sample shows a clear glass transition, followed by an extended supercooled liquid region and a multi-stage crystallization process as the temperature increases. The value of the glass transition temperature (T_g), the crystallization temperature (T_x), the supercooled liquid region ($\Delta T = T_x - T_g$) and the total crystallization enthalpy (ΔH_x) of the sample are 681 K, 723 K, 42 K and 180.2 J/g, respectively. The DSC result further confirms the fully glassy structure of the present sample. Noticeably, the ΔT_x of the alloy, one of the important parameters in evaluating glass forming ability (GFA), are larger than that of the reported HE-BMGs [14,15], indicating their good GFA.

Fig. 2 shows the temperature dependence of the magnetization curves of the $\text{Fe}_{25}\text{Co}_{25}\text{Ni}_{25}\text{Mo}_5\text{P}_{10}\text{B}_{10}$ HE-BMG under 0.02 T. By deriving the M - T curve to obtain the dM/dT - T curve shown in the inset of Fig. 2, the Curie temperature (T_C) of the sample can be determined to be 560 K. Fig. 3 shows the isothermal magnetization curves of the $\text{Fe}_{25}\text{Co}_{25}\text{Ni}_{25}\text{Mo}_5\text{P}_{10}\text{B}_{10}$ HE-BMG under various applied fields up to 5 T

in the temperature range of 430–650 K, in which the test temperature interval is 5 K near the Curie temperature and 10 K away from the Curie temperature. It can be seen that the magnetization of the sample achieves saturation at low applied magnetic fields when the test temperature is below T_C , while the M - H curves of the sample become linear when the test temperature is near and above T_C , indicating the transitions from ferromagnetic state to paramagnetic state. The magnetic entropy change (ΔS_M), which is usually used to characterize the magnetocaloric effect of the materials, can be calculated from magnetization isotherms using the Maxwell relation [17]:

$$\Delta S_M(T, H) = \int_0^{H_{\max}} \left(\frac{\partial M}{\partial T} \right)_H dH \quad (1)$$

where H_{\max} is the maximum applied field. In fact, ΔS_M is usually calculated based on the following alternative equation [17]:

$$\Delta S_M(T_i, H) = \frac{\int_0^H M(T_i, H) dH - \int_0^H M(T_{i+1}, H) dH}{T_i - T_{i+1}} \quad (2)$$

Fig. 4 shows the temperature dependence of $-\Delta S_M$ of the $\text{Fe}_{25}\text{Co}_{25}\text{Ni}_{25}\text{Mo}_5\text{P}_{10}\text{B}_{10}$ HE-BMG under 1–5 T calculated by Eq. (2). It can be determined from Fig. 4 that the peak value ($|\Delta S_M^{\text{peak}}|$) and the full width at half maximum (ΔT_{FWHM}) of the $|\Delta S_M|$ peak are $0.80 \text{ J kg}^{-1} \text{ K}^{-1}$ and 169 K under the applied magnetic field of 1.5 T, $1.88 \text{ J kg}^{-1} \text{ K}^{-1}$

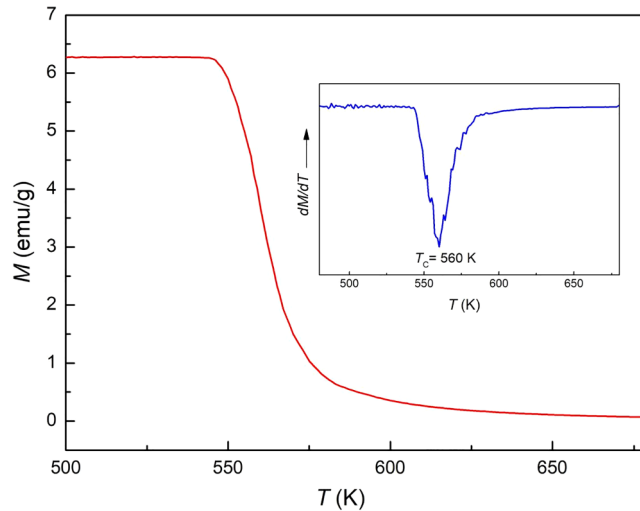


Fig. 2. Temperature dependence of the magnetization and dM/dT versus temperature curves for $\text{Fe}_{25}\text{Co}_{25}\text{Ni}_{25}\text{Mo}_5\text{P}_{10}\text{B}_{10}$ HE-BMG under 0.02 T.

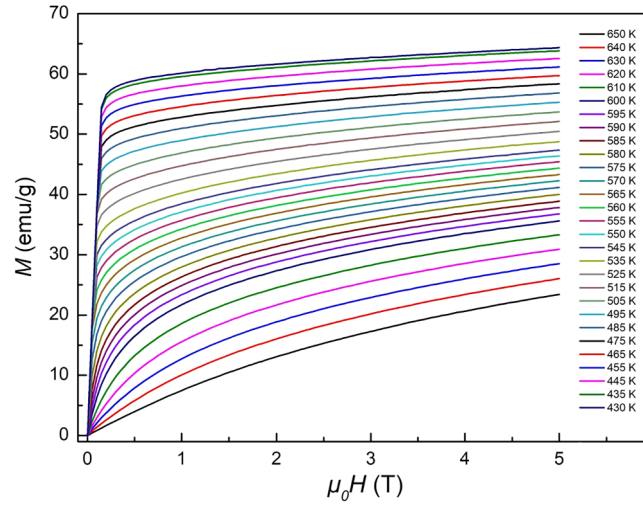


Fig. 3. Isothermal magnetization curves of $\text{Fe}_{25}\text{Co}_{25}\text{Ni}_{25}\text{Mo}_5\text{P}_{10}\text{B}_{10}$ HE-BMG measured in the temperature range from 430 K to 650 K.

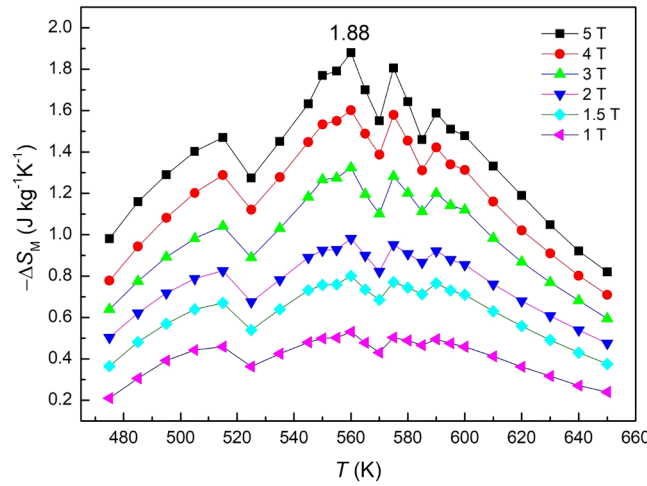


Fig. 4. Magnetic entropy changes as a function of temperature under the applied magnetic field of 1–5 T for the present $\text{Fe}_{25}\text{Co}_{25}\text{Ni}_{25}\text{Mo}_5\text{P}_{10}\text{B}_{10}$ HE-BMG.

Table 1

Magnetocaloric properties of the present $\text{Fe}_{25}\text{Co}_{25}\text{Ni}_{25}\text{Mo}_5\text{P}_{10}\text{B}_{10}$ HE-BMG and some selected transition metal-based BMGs at the different applied magnetic field.

Composition (at.%)	T_C (K)	$ \Delta S_M^{\text{peak}} $ ($\text{J kg}^{-1}\text{K}^{-1}$)			RC (J kg^{-1})			ΔT_{FWHM} ($\text{J kg}^{-1}\text{K}^{-1}$)	Ref.
		1.5T	2T	5T	1.5T	2T	5T		
$\text{Fe}_{80}\text{P}_{13}\text{C}_7$	579	2.20	2.7	5.05	125.6	170.1	479.8	95	[16]
$\text{Fe}_{79}\text{Gd}_1\text{B}_{12}\text{Cr}_8$	355	1.42	3.59		153		627		[25]
$\text{Fe}_{77}\text{Ta}_3\text{B}_{10}\text{Zr}_9\text{Cu}_1$	313		1.04	2.03		92.2	241.5		[23]
$\text{Fe}_{66}\text{Mn}_{14}\text{P}_{10}\text{B}_7\text{C}_3$	319	0.91	1.12		99.84	134.3			[27]
$\text{Co}_{71}\text{Mo}_9\text{P}_{14}\text{B}_6$	317	0.37	0.47	0.96	33.0	41.3	70.5	72.9	[24]
$\text{Co}_{62}\text{Nb}_6\text{Zr}_2\text{B}_{30}$	210	0.36							[28]
$\text{Fe}_{25}\text{Co}_{25}\text{Ni}_{25}\text{Mo}_5\text{P}_{10}\text{B}_{10}$	560	0.80	0.98	1.88	135.4	169.9	310.2	165	present

K^{-1} and 165 K under the applied magnetic field of 5 T, respectively. The refrigeration capacity (RC) is another relevant parameter to characterize the efficiency of magnetic refrigerant. The RC corresponds to the area of the $-\Delta S_M$ curve and can be simply estimated by multiplying the $|\Delta S_M^{\text{peak}}|$ and ΔT_{FWHM} of the $-\Delta S_M$ curve. So, the RC of the $\text{Fe}_{25}\text{Co}_{25}\text{Ni}_{25}\text{Mo}_5\text{P}_{10}\text{B}_{10}$ HE-BMG can be estimated to be 135.4 J kg^{-1} and 310.2 J kg^{-1} under the applied magnetic field of 1.5 T and 5 T, respectively. Table 1 lists the magnetocaloric properties of the present $\text{Fe}_{25}\text{Co}_{25}\text{Ni}_{25}\text{Mo}_5\text{P}_{10}\text{B}_{10}$ HE-BMG and some selected transition metal-based BMGs under different applied magnetic fields. Compared with other TM-based BMGs, the magnetocaloric properties of the present

$\text{Fe}_{25}\text{Co}_{25}\text{Ni}_{25}\text{Mo}_5\text{P}_{10}\text{B}_{10}$ HE-BMG are not outstanding. The value of $|\Delta S_M^{\text{peak}}|$ of the present $\text{Fe}_{25}\text{Co}_{25}\text{Ni}_{25}\text{Mo}_5\text{P}_{10}\text{B}_{10}$ HE-BMG is higher than that of Co-based BMGs, but lower than that of Fe-based BMGs.

It is known that the value of $|\Delta S_M^{\text{peak}}|$ of an alloy is proportional to its saturation magnetization (J_s) [26]. The plot of J_s against $|\Delta S_M^{\text{peak}}|$ under the applied magnetic field of 1.5 T of the present $\text{Fe}_{25}\text{Co}_{25}\text{Ni}_{25}\text{Mo}_5\text{P}_{10}\text{B}_{10}$ HE-BMG together with several selected TM-based BMGs is shown in Fig. 5. The data points corresponding to these transition metal-based BMGs in Fig. 6 are linearly fitted by the least squares method and the R-square of the fitted straight line is 0.936, indicating a good linear relationship between the J_s and $|\Delta S_M^{\text{peak}}|$. The

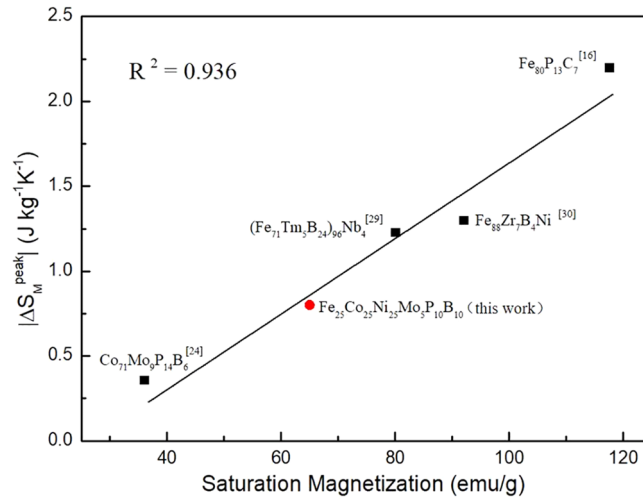


Fig. 5. Plot of saturation magnetization against $|\Delta S_M^{\text{peak}}|$ of the present $\text{Fe}_{25}\text{Co}_{25}\text{Ni}_{25}\text{Mo}_5\text{P}_{10}\text{B}_{10}$ HE-BMG and several selected transition metal-based BMGs under the applied magnetic field of 1.5 T [16,23,29,30].

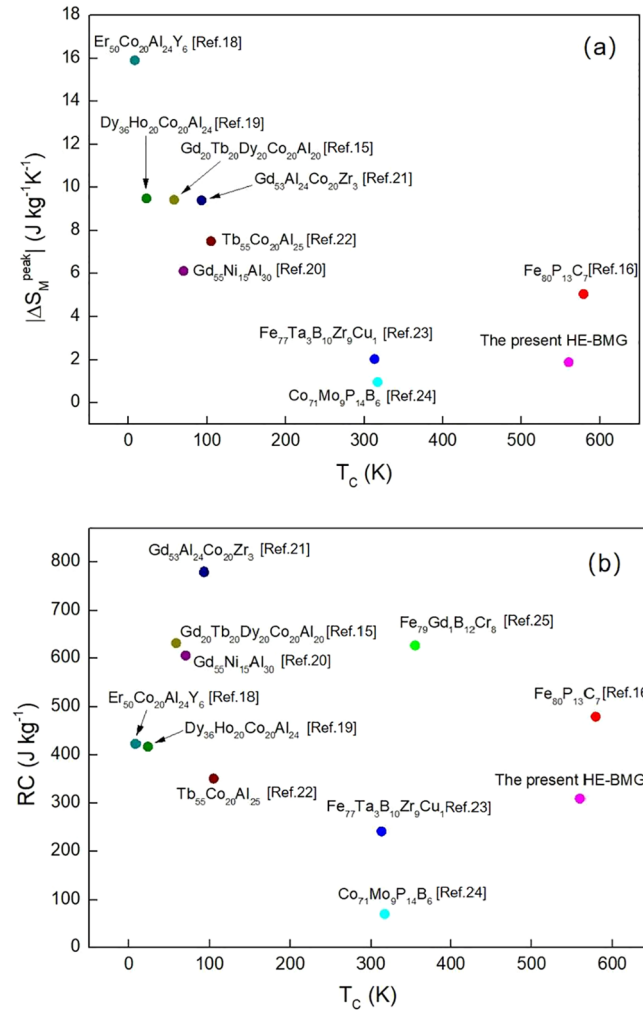


Fig. 6. The relationship between the Curie temperature (T_c) and the magnetic entropy change ($|\Delta S_M^{\text{peak}}|$) (a) and refrigeration capacity (RC) (b) under a magnetic field of 5 T of some typical magnetocaloric amorphous alloys [15,16,18–24].

present $\text{Fe}_{25}\text{Co}_{25}\text{Ni}_{25}\text{Mo}_5\text{P}_{10}\text{B}_{10}$ HE-BMG also follows this linear relationship, which seems to suggest that the high entropy effect does not contribute to the $|\Delta S_M^{\text{peak}}|$ of metallic glasses. However, it can be found from Table 1 that the present $\text{Fe}_{25}\text{Co}_{25}\text{Ni}_{25}\text{Mo}_5\text{P}_{10}\text{B}_{10}$ HE-BMG has a

much larger ΔT_{FWHM} compared to the other transition metal-based BMGs, indicating that the high entropy effect may widen the magnetic transition temperature range of the present transition metal-based HE-BMG. This feature had also been found in Gd-Tb-Dy-Al-M ($M = \text{Fe}, \text{Co}$,

Ni) high-entropy amorphous alloys, in which the authors attribute this result to the amorphous spin glass behavior and the complex composition of high-entropy amorphous alloys [15]. So, although the high entropy effect has no positive effect on the value of T_c , it leads to a wide ΔT_{FWHM} , thus a high RC of the present $\text{Fe}_{25}\text{Co}_{25}\text{Ni}_{25}\text{Mo}_5\text{P}_{10}\text{B}_{10}$ $|\Delta S_M^{\text{peak}}|$ HE-BMG as shown in Table 1.

Fig. 6 shows the $|\Delta S_M^{\text{peak}}|$ and RC as a function of T_c under a magnetic field of 5 T of some typical RE-based and TM-based magnetocaloric amorphous alloys. It is seen that the present $\text{Fe}_{25}\text{Co}_{25}\text{Ni}_{25}\text{Mo}_5\text{P}_{10}\text{B}_{10}$ HE-BMG has larger values of $|\Delta S_M^{\text{peak}}|$ and RC among TM-based amorphous alloys. Compared with TM-based amorphous alloys, RE-based amorphous alloys exhibit the larger values of $|\Delta S_M^{\text{peak}}|$ and RC. However, RE-based amorphous alloys generally have the very low T_c , and thus is only suitable for low temperature magnetic refrigeration. The present $\text{Fe}_{25}\text{Co}_{25}\text{Ni}_{25}\text{Mo}_5\text{P}_{10}\text{B}_{10}$ HE-BMG exhibits a high magnetic transition temperature, which has potential to be used as room-temperature magnetocaloric materials through composition tuning. Room-temperature magnetocaloric materials can be used for domestic refrigerators, air conditions and other refrigeration devices, and thus has great practical value and research significance.

4. Conclusion

The $\text{Fe}_{25}\text{Co}_{25}\text{Ni}_{25}\text{Mo}_5\text{P}_{10}\text{B}_{10}$ HE-BMG with a maximum diameter of 1.2 mm has been prepared by combining fluxing treatment and J-quenching technique. The Curie temperature of the present $\text{Fe}_{25}\text{Co}_{25}\text{Ni}_{25}\text{Mo}_5\text{P}_{10}\text{B}_{10}$ HE-BMG is 560 K. The values of $|\Delta S_M^{\text{peak}}|$ and RC of the present $\text{Fe}_{25}\text{Co}_{25}\text{Ni}_{25}\text{Mo}_5\text{P}_{10}\text{B}_{10}$ HE-BMG are $0.801 \text{ J kg}^{-1} \text{ K}^{-1}$ and 135.37 J kg^{-1} under 1.5 T, and $1.88 \text{ J kg}^{-1} \text{ K}^{-1}$ and 310.20 J kg^{-1} under 5 T, respectively. Our results suggest that the high entropy effect seems to have little effect on the value of $|\Delta S_M^{\text{peak}}|$, but obviously broadens the ΔT_{FWHM} of the ΔS_M peak, thus resulting in a higher refrigeration capacity of the present $\text{Fe}_{25}\text{Co}_{25}\text{Ni}_{25}\text{Mo}_5\text{P}_{10}\text{B}_{10}$ HE-BMG.

Acknowledgements

This research was sponsored by National Natural Science Foundation of China (Grant Nos. 51561028, 51771161 and 51771217) and Zhejiang Provincial Natural Science Foundation of China (No. LY17E010005).

References

- [1] C.J. Byrne, M. Eldrup, Materials science. Bulk metallic glasses, *Science* 321 (5888) (2008) 502–503.
- [2] X.Y. Liu, et al., Thermomagnetic properties of amorphous rare-earth alloys with Fe, Ni, or Co, *J. Appl. Phys.* 79 (3) (1996) 1630–1641.
- [3] E.P. Nobrega, et al., Theoretical investigation on the magnetocaloric effect in amorphous systems, application to: $\text{Gd}_{80}\text{Au}_{20}$ and $\text{Gd}_{70}\text{Ni}_{30}$, *J. Appl. Phys.* 113 (24) (2013) 366.
- [4] M. Foldeaki, et al., Effect of sample preparation on the magnetic and magnetocaloric properties of amorphous $\text{Gd}_{70}\text{Ni}_{30}$, *J. Appl. Phys.* 83 (5) (1998) 2727–2734.
- [5] Chang, et al., Microstructural development in equiatomic multicomponent alloys, *Mater. Sci. Eng. A* 375–377 (1) (2004) 213–218.
- [6] J.-W. Yeh, et al., Nanostructured high-entropy alloys with multiple principal elements: novel alloy design concepts and outcomes, *Adv. Eng. Mater.* 6 (5) (2004) 299–303.
- [7] J.Y. He, et al., Effects of Al addition on structural evolution and tensile properties of

- the FeCoNiCrMn high-entropy alloy system, *Acta Mater.* 62 (1) (2014) 105–113.
- [8] S. Singh, et al., Decomposition in multi-component AlCoCrCuFeNi high-entropy alloy, *Acta Mater.* 59 (1) (2011) 182–190.
- [9] H.F. Li, et al., In vitro and in vivo studies on biodegradable CaMgZnSrYb high-entropy bulk metallic glass, *Acta Biomater.* 9 (10) (2013) 8561–8573.
- [10] H.Y. Ding, K.F. Yao, High entropy $\text{Ti}_{20}\text{Zr}_{20}\text{Cu}_{20}\text{Ni}_{20}\text{Be}_{20}$ bulk metallic glass, *J. Non-Crystalline Solids* 364 (2013) 9–12.
- [11] K. Zhao, et al., Room temperature homogeneous flow in a bulk metallic glass with low glass transition temperature, *Appl. Phys. Lett.* 98 (14) (2011) 4067.
- [12] X.Q. Gao, et al., High mixing entropy bulk metallic glasses, *J. Non-Crystalline Solids* 357 (21) (2011) 3557–3560.
- [13] Ka Gschneidner Jr., Y. Mudryk, D. Paudyal, Making the most of the magnetic and lattice entropy changes, *J. Magnet. Magnet. Mater.* 321 (21) (2009) 3541–3547.
- [14] Juntao Huo, et al., High-entropy bulk metallic glasses as promising magnetic refrigerants, *J. Appl. Phys.* 117 (7) (2015) 1479.
- [15] Juntao Huo, et al., The magnetocaloric effect of Gd-Tb-Dy-Al-M (M = Fe, Co and Ni) high-entropy bulk metallic glasses, *Intermetallics* 58 (58) (2015) 31–35.
- [16] Weiming Yang, et al., Extraordinary magnetocaloric effect of Fe-based bulk glassy rods by combining fluxing treatment and J-quenching technique, *J. Alloy. Compd.* 684 (2016) 29–33, <https://doi.org/10.1016/j.jallcom.2016.05.142>.
- [17] T. Hashimoto, et al., Magnetic refrigeration in the temperature range from 10 K to room temperature: the ferromagnetic refrigerants, *Cryogenics* 21 (11) (1981) 647–653.
- [18] Q. Luo, et al., Magnetocaloric effect of Ho-, Dy-, and Er-based bulk metallic glasses in helium and hydrogen liquefaction temperature range, *Appl. Phys. Lett.* 90 (21) (2007) 867.
- [19] L. Liang, et al., An Er-based bulk metallic glass with high thermal stability and excellent magnetocaloric properties, *Intermetallics* 463.1 (2008) 30–33.
- [20] Fang Yuan, J. Du, B. Shen, Controllable spin-glass behavior and large magnetocaloric effect in Gd-Ni-Al bulk metallic glasses, *Appl. Phys. Lett.* 101 (3) (2012), 2045.
- [21] Q. Luo, et al., Magnetocaloric effect in Gd-based bulk metallic glasses, *Appl. Phys. Lett.* 89 (8) (2006), 081914.
- [22] J. Du, et al., Spin-glass behavior and magnetocaloric effect in Tb-based bulk metallic glass, *J. Magn. Magn. Mater.* 321 (5) (2009) 413–417.
- [23] X.C. Zhong, et al., Thermal, magnetic and magnetocaloric properties of $\text{Fe}_{80-x}\text{Mx}\text{B}_{10}\text{Zr}_9\text{Cu}_1$ (M = Ni, Ta; x = 0, 3, 5) amorphous alloys, *J. Alloys Compd.* 633 (2005) 188–193.
- [24] Cong Liu, et al., Near room-temperature magnetocaloric effect of Co-based bulk metallic glass, *J. Magnet. Magnet. Mater.* 446 (2017).
- [25] J.Y. Law, R.V. Ramanujan, V. Franco, Tunable Curie temperatures in Gd alloyed Fe–B–Cr magnetocaloric materials, *J. Alloy. Compd.* 508 (1) (2010) 14–19.
- [26] K.A. Gschneidner Jr., V.K. Pecharsky, Magnetocaloric materials, *Annu. Rev. Mater. Res.* 30 (1) (2000) 387–429.
- [27] Huiyan Zhang, et al., Near, room-temperature magnetocaloric effect in FeMnPBC metallic glasses with tunable Curie temperature, *J. Magn. Magn. Mater.* 347 (12) (2013) 131–135.
- [28] L.M. Moreno, et al., Magnetocaloric effect of $\text{Co}_{62}\text{Nb}_6\text{Zr}_2\text{B}_{30}$ amorphous alloys obtained by mechanical alloying or rapid quenching, *J. Appl. Phys.* 115 (17) (2014) 1653.
- [29] Jiawei Li, et al., Magnetocaloric effect of Fe–RE–B–Nb (RE = Tb, Ho or Tm) bulk metallic glasses with high glass-forming ability, *J. Alloys Compd.* 644 (2015) 346–349.
- [30] Xingzhou Li, P. Ye, Magnetocaloric effect in Fe–Zr–B–M (M = Ni, Co, Al, and Ti) amorphous alloys, *J. Appl. Phys.* 116.9 (2014) 305.

Kenan Wu^a, Cong Liu^a, Qiang Li^{a,*}, Juntao Huo^{b,*}, Mingcan Li^a,
Chuntao Chang^{c,a}, Yanfei Sun^a

^a School of Physics Science and Technology, Xinjiang University, Urumqi, Xinjiang 830046, People's Republic of China

^b CAS Key Laboratory of Magnetic Materials and Devices, Ningbo Institute of Materials Technology & Engineering, Chinese Academy of Sciences, Ningbo, Zhejiang 315201, People's Republic of China

^c School of Mechanical Engineering, Dongguan University of Technology, Dongguan 523808, People's Republic of China
E-mail addresses: qli@xju.edu.cn (Q. Li),
huojuntao@nimte.ac.cn (J. Huo).

* Corresponding authors.